Little Balls of Stress: Understanding the Activation Pathway of Resveratrol-Induced Stress Granules

A Major Qualifying Project

Submitted to the Faculty of

Worcester Polytechnic Institute

in partial fulfillment of the requirements for the

Degree of Bachelor of Science

In

Biology and Biotechnology

Submitted by:

_____

Katherine Stratton

Date: January 24th, 2022

Project Advisor:

_____

Professor Natalie Farny

Abstract

When eukaryotic cells experience short-term stressors, they may produce stress granules (SGs) through the phosphorylation of translational regulator eIF2α in the integrated stress response (ISR) pathway. The ISR is triggered by one of four specialized kinases reacting to stressors. Resveratrol—a stilbene produced by several plants in response to stress—has been hypothesized to produce SGs in eukaryotes through the phosphorylation reaction in the ISR. The goal of this project was to confirm if eIF2α phosphorylation is required for resveratrol-induced SG formation, and which kinase reacts to Rsv to form SGs. Using fluorescence microscopy, SG presence was scored in two separate Rsv acute exposure assays using MEFs: the first used an eIF2α S51A mutant that inactivated eIF2α phosphorylation to determine if Rsv SGs are eIF2α-dependent, and the second used PERK and HRI kinase knockouts to examine which kinase reacts to Rsv to trigger the ISR. It was found that Rsv-induced SGs are eIF2α dependent and formed through the involvement of the PERK ISR kinase.

Acknowledgements

My advisor *Professor Natalie Farny* for her limitless and unconditional support during this project. Her positive attitude and kind guidance were invaluable throughout the research and writing process and has inspired me to not only continue seeking a career in biology and cell culture, but to also strive for a positive outlook on life. I'm so thankful to have had the opportunity to work with her this school year, and will remember the experience for the rest of my life.

Dr. Nancy Kedersha and Dr. Paul Anderson of Brigham and Women's Hospital in Boston, MA for donating the MEF-WT, MEF-S51A, MEF-ΔPERK, and MEF-ΔHRI cell lines, without which the project would not have been possible.

Worcester Polytechnic Institute Department of Biology and Biotechnology for providing the space, supplies, and equipment.

Table of Contents

Introduction

Integrated Stress Response and Stress Granule Formation

The Integrated Stress Response (ISR) is a cellular response that mammalian cells perform when exposed to external stressors, such as viral infection, oxidative stress, and nutrient deficiencies (Anderson & Kedersha, 2009). This response is triggered as a survival method, allowing the cell to react to stressors that could potentially damage its DNA, proteins, or cellular macromolecules. Depending on the severity and duration of exposure to the toxin, the pathway provokes a cytoprotective or cytotoxic response. A cytoprotective stress response repairs the damage inflicted and lets the cell continue its main function, while a cytotoxic response initiates cellular apoptosis (Fulda et al., 2010). These cytoprotective and cytotoxic mechanisms can lead to the formation of stress granules, depending on the stressor applied, the type of cell experiencing the stress, and the context and duration of stress exposure.

Stress granules (SGs) are membraneless cytoplasmic ribonucleoprotein (RNP) assemblies that form to conserve cellular energy when repairing damage caused by stress. SGs contain components relating to mRNA translation, such as untranslated mRNAs, ribosomal components, translation initiation factors, and RNA-binding proteins (Campos-Melo et al., 2021). These components are sequestered within SGs to conserve cellular energy and resources used during translation and protein synthesis, halting any translation deemed unnecessary for cell survival so the cell may respond to and heal from environmental stressors. By suppressing unnecessary protein synthesis there are more resources and energy available for the cell to defend and repair from extracellular stress, increasing the cell's odds of survival (Matsuki et al., 2012).

The ISR pathway leads to SG formation, triggered by one of four specific kinases: PERK, PKR, HRI, or GCN2. Each kinase retains relative homology between their eIF2α kinase sites, however their unique regulatory mechanisms allow them to respond to different environmental and physiological stressors (Anderson & Kedersha, 2009). Once exposed to their specific stressor, the target kinase fully activates through dimerization and autophosphorylation, which in turn leads to the phosphorylation of the eukaryotic initiation factor protein eIF2, specifically at serine51 of the alpha subunit. The increased levels of phosphorylated eIF2α inhibits translation initiation of nearly all proteins, except for those designed to control cell adaptation to stress (Darini et al., 2019). The incomplete proteins and untranslated mRNAs not involved in stress adaptation are then sequestered within the cell's cytoplasm, forming SGs. While all four kinases

can induce SGs and promote either cell death or survival, kinase PKR specifically encourages apoptosis and cell death (Koromilas, 2019).

Resveratrol and its Effect on SG Formation

Resveratrol (Rsv) is a phenolic stilbene compound highly studied for its several potential health benefits. The compound is produced in plants as a response to cellular injury or stressors and was first discovered in the skins of grapes (Frémont, 2000). It can also be found in several other foods, from grape products like red wine, to other plants like blueberries and peanuts, and even in dark chocolate (Langcake & Pryce, 1976). The structure of resveratrol is comprised of two aromatic rings connected by a styrene double bond (Frémont, 2000). The cis and trans isomers of resveratrol are shown below in Figure 1.

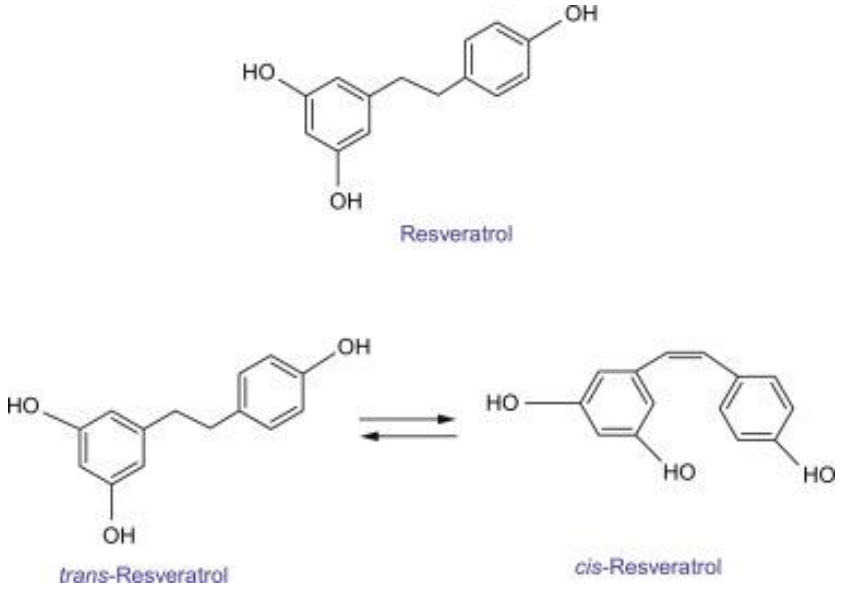

Figure 1. Structures of Isometric *cis*- and *trans*- states of resveratrol. Adapted from "Chemopreventative role of dietary phytochemicals in colorectal cancer," by Bansal et al., 2018, *Advances in Molecular Toxicology, 12*. Copyright 2018 by ScienceDirect.

Resveratrol as a treatment has been studied in conjunction with a variety of different diseases, from chronic and inflammatory illnesses to even cancer. It is highly studied especially by cancer researchers due to its ability to induce apoptosis in several cancer cell lines such as leukemia and neuroblastoma cells (Takashina et al., 2017; Pizarro et al., 2011). Resveratrol has also been hypothesized to possess anti-oxidative, anti-inflammatory, and anti-atherogenic properties (Piotrowska et al., 2012).

Rsv triggers the ISR when exposed at very high concentrations to eventually produce SGs by upregulating phosphorylation of eIF2 at serine 51 of the alpha subunit (eIF2α). Phosphorylating eIF2α blocks the exchange of GDP to GTP on the protein, which inhibits the eIF2 complex from delivering transfer RNAs (tRNAs) to start codons. This has the overall effect of reducing the amount of energy available to the cell and downregulating translation initiation, resulting in translational control (Villa-Cuestra et al., 2011). Some hypothesize that Rsv induces the ISR by binding to G3BP1 (Amen et al., 2021), which is a key protein required for the formation of SGs (Tourrière et al., 2003; Kedersha et al., 2016).

Project Rationale and Objectives

A previous research project explored the relationship between Rsv SGs and initiation factor eIF2α using HAP1 cells. They performed acute exposure assays with Rsv using a wildtype and S51A replacement mutation HAP1 cell lines, as well as four mutant knockout cell lines that removed one of the four ISR kinases. Through their study, the project team concluded that Rsv-induced SGs are eIF2α-dependent and proposed that kinase PERK is involved in the phosphorylation of eIF2α (Milks et al., 2022). However, the choice of cell line may have influenced their results.

HAP1 cells are a near-haploid cell line derived from the KBM7 near-haploid cell line, which originated from a human male with chronic myelogenous leukemia (Beigl et al., 2020). HAP1 cells are loosely adherent, meaning they adhere to the bottom of a culture flask, but some lift up from the monolayer. Their loose adherence and morphology makes imaging HAP1 cells difficult, as they would often fall off of coverslips during the fixation and staining process, leading to complications in interpreting microscopy results. By using a more tightly adherent cell line such as Mouse Embryonic Fibroblasts (MEFs), analyzing the cells on a microscope slide becomes easier due to the cell type's stronger adherence and distinct morphology nature to adhere to the bottom of a culture flask in a monolayer and to drastically change in morphology when dead.

The purpose of this study is to repeat the HAP1 acute exposure experiment using adherent MEF cell lines. This change adds confidence and increases the rigor of the study through repeating the experiment in different cell lines (HAP1 vs. MEF) derived from different species (human vs. mice). Also, the knockouts were generated through two different methods,

with the MEF knockout lines generated through conventional mouse knockout generation by way of homologous recombination, and the HAP1 knockouts through the newer technology of CRISPR-KO. These changes add certainty to the roles of eIF2α and PERK in modulating the ISR response to Rsv in mammalian cells.

Materials and Methods

Cell Line Maintenance

Four embryonic derived MEF cell lines were used to investigate stress granule formation in response to resveratrol: wildtype, mutant S51A, ΔPERK, and ΔHRI. These cells were a kind gift from Drs. Paul Anderson and Nancy Kedersha of Brigham and Women's Hospital in Boston, Massachusetts. MEF (mouse embryonic fibroblast) cell lines were derived from mouse embryos after 13 days of embryonic development. This mammalian cell line has adherent properties, anchoring to the bottom of the culture flask and forming a monolayer during incubation (Scheuner et al., 2001; Harding et al., 2000; Han et al., 2001). Dulbecco's Modified Eagle Medium (DMEM) was used to maintain the MEF cells with 10% Fetal Bovine Serum (FBS), 1% penicillin/streptomycin (P/S), and 1% sodium pyruvate. The S51A mutant culture also had 1% non-essential amino acids added to their growth media. Initially the ΔHRI cells were cultured in the same medium with 20% FBS concentration due to the fragile nature of the thawed cells. The cells were incubated at 37˚C and checked every 2-3 days, split 1:3, 1:6, or 1:8 depending on when the cells reached 90% confluency.

Acute Drug Exposure Assay: eIF2α Dependence and Pathway Confirmation

MEF wild-type cells and S51A mutant cells were exposed to 500uM of Rsv, EtOH and Ars. 18mm round sterile glass coverslips were placed in the bottom of the first two rows of wells of a 12-well plate. The cells were plated at a concentration of 1 X 10^5 cells per well. 1mL of suspended cells were added to each of the 8 wells used, then incubated for 24 hours at 37 degrees C to allow the cells to adhere to the coverslips. After examining the plate wells to confirm proper cell growth, 500uL of media was removed from each well and added to 1.5mL Eppendorf tubes. The corresponding volumes of treatment (EtOH for negative control, Arsenite for positive control, and Rsv as the test condition) were added to each treatment tube as seen in Figure 1 below, then added back to the corresponding wells. The "untreated" condition did not have any media removed and was left untouched during the application of treatments. After 1 hour of incubation, the media was removed and washed with 1x PBS. To not disturb the cells on the cover slips, the well plates were tipped 45 degrees and the aspirator tip placed in the well volume away from the cover slip. Once washed, 500uL of 4% paraformaldehyde in PBS was added to each well to fix the cells together, then 500uL of 100% methanol post-fixing solution removal.

The plate was shaken for 10 minutes between each step. Wells were then washed again with 1x PBS to remove the last of the methanol and prepare the cells for immunoassay antibody staining.

To confirm what kinase triggers ISR pathway stress granule formation in response to Rsv, a second acute exposure assay was performed using the MEF wild type, ΔHRI, and ΔPERK cell lines. The MEF WT cells were plated in its well column at the same density as above. MEF ΔPERK, due to the cell line's increased doubling time compared to the other cell lines, were plated at 0.5 x 10^5 cells well to not have the cover slips get overgrown. ΔHRI were plated at as close to 1 x 10^5 cells/well as possible, due to the cells' fragility and decreased growth rate. Once plated, the cells were treated and fixed as described above, and outlined in Figure 2.

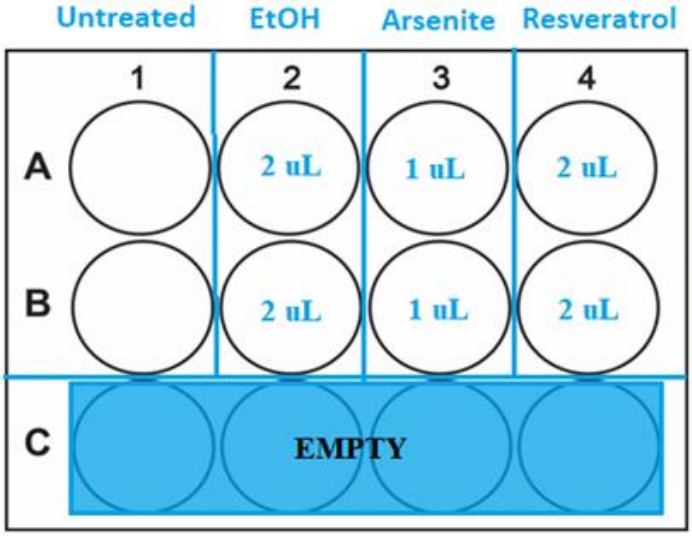

Condition	Starting Concentration	Concentration Used
100% Ethanol	Pure	500 µM
Arsenite	0.5 mM	500 µM
Resveratrol	0.25 mM	500 µM

Figure 2. Schematic of experimental setup used for acute exposure assays. MEF wild-type, S51A, ΔHRI, and ΔPERK acute exposure assay (left), and a table detailing the concentrations of the used treatments (right).

Immunofluorescence Assay: Antibody Staining

After fixation, a fluorescence immunoassay was performed on each well. Each well was treated with 500uL of 5% bovine serum albumin (BSA) in PBS blocking solution and placed on a rotator table for 1-2 hours. Once the blocking solution was removed, 500uL of the primary antibody solution was added to the cells and incubated on a rotator table at room temperature for one hour, or at 4˚C for 24 hours. The purpose of the primary antibody is to detect the G3BP1 proteins contained within SGs and bind to said protein. The primary antibody solution was then removed and all wells were washed three times for 5 minutes each with 1x PBS. When the last

wash was removed, 500uL of the secondary antibody solution was added to each well, and the plate was incubated again for one hour at room temperature on a rotator table, covering the plate with tinfoil to prevent photobleaching the fluorescent secondary antibody. The components and dilutions of each antibody solution are shown in Table 1 below. The wells were washed again (3 times for 5 minutes each) after incubation, leaving the final wash in the wells.

Table 1. Table of antibody solution components used to stain cells for Fluorescence Microscopy

Component	Application	Dilution	Manufacturer	Product #
Rabbit-anti-G3BP1	1˚ antibody stain	1:2000	Proteintech	13057-2-AP
Anti-rabbit IgG Cy2 (green) stain	2˚ antibody stain	1:1000	Jackson Immunoresearch	711-225-152
Hoscht 3342 nuclear stain	DNA stain	1:5000	Life Technologies	1642791
Mouse-anti-G3BP1	1˚ antibody stain	1:2000	Proteintech	66486-1-Ig
Anti-mouse IgG Alexa Flour 488 stain	2˚ antibody stain	1:1000	Jackson Immunoresearch	715-545-150

Mounting Coverslips and Sample Analysis

The coverslips were mounted on glass microscope slides cells-side down in warmed Polyvinyl alcohol mounting media. The coverslips were removed from the plate wells containing the final secondary antibody wash using two pairs of needle nose tweezers, and then pressed into the mounting media with a folded KimWipe, removing the excess media. The slides were then gently rinsed with distilled sterile water in a squirt bottle to remove the last of the excess mounting media and dabbed dry once more.

Once mounted and dried, the slides were placed in a slide folder at room temperature to cure for at least 10 minutes. Slides were then blinded using colored tape to remove bias during analysis and placed under an inverted fluorescence microscope. Cells were analyzed by observing at least three fields containing cells, counting at least 250 cells total per slide. Two different infinity corrected objective lenses were used, on a Zeiss Observer A1 microscope: a 40X magnification lens, and a 63X oil immersion lens. The cells counted were classified as

positive or negative for displaying G3BP1-containing SGs, and the percentage of cells positive for SGs was determined per sample.

Results

Resveratrol-Induced Stress Granules in MEFs are eIF2α Dependent

An acute exposure assay was performed on MEF WT and MEF S51A cells to determine the percentage of cells forming SGs in response to ethanol (negative control), Arsenite (positive control), Rsv, or no treatment. This was to determine if the formation of SGs in MEF cells are dependent on the phosphorylation of eIF2α. S51A mutant cells were used because the ser/ala amino acid replacement in eIF2α makes the protein unable to phosphorylate, thus disrupting the ISR pathway (Sheuner et al., 2001). Each cell was scored using a fluorescence microscope, with a positive response indicated by small, green, fluorescent dots dispersed throughout the cytoplasm of the cell. A negative response resulted in the cell being diffusely green throughout the cytoplasm, with an occasional green marker where the fluorescent antibody was not completely washed away, seen in the S51A untreated cell in Figure 3 below. The concentrations of Ars and Rsv used were extrapolated from a previous MQP study on the same subject (Milks et al., 2022).

The SGs formed from arsenite exposure were significantly larger than those from Rsv, indicated in the WT example cells in Figure 3. While the WT MEF cells formed SGs in response to acute Ars and Rsv exposure, the S51A MEFs did not form SGs in response to either treatment (Figure 3).

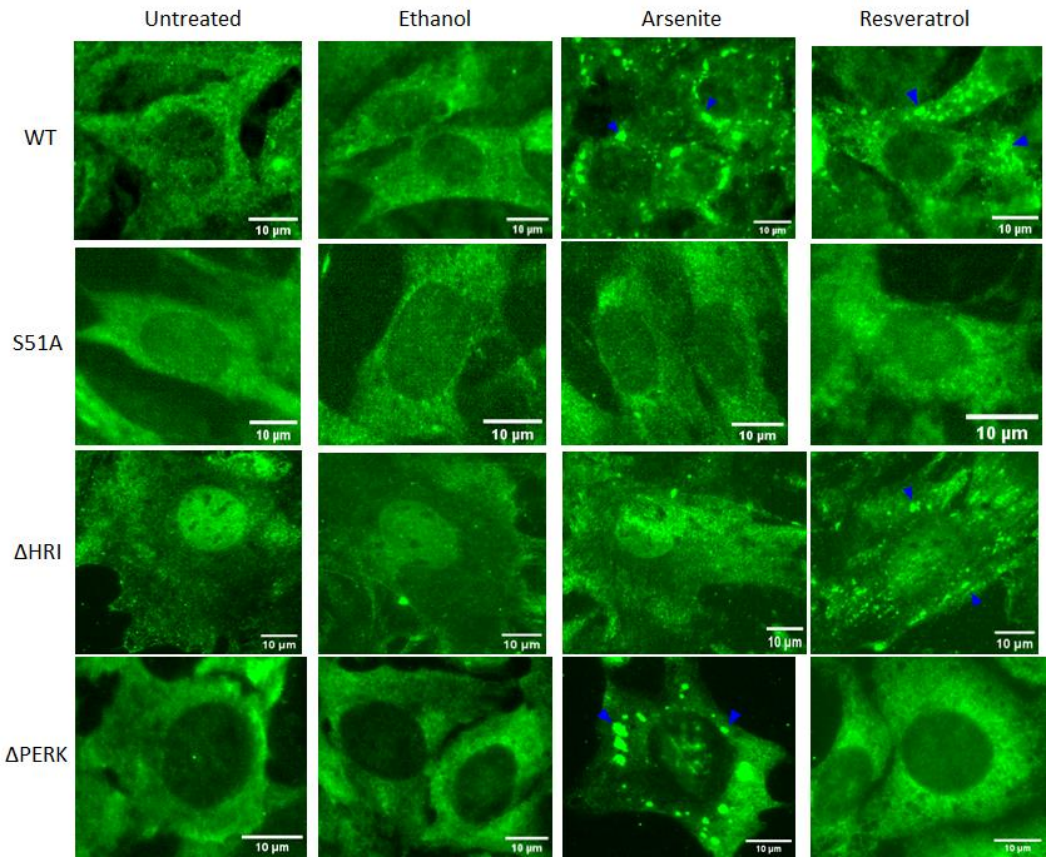

Figure 3. Representative images of MEF WT, S51A, ΔHRI, and ΔPERK cells after acute exposure assay and immunostaining. SG positive signal indicated with blue arrows. Note that only Arsenite-treated WT and ΔPERK cells and Rsv-treated WT and ΔHRI cells produced SGs. All scale bars are 10 microns in length.

To determine if SGs formed due to Rsv exposure are eIF2α-dependent, MEF WT and MEF S51A cells were evaluated for SG formation after being acutely exposed to the treatments and immunostained for G3BP1. The average percentage of cells positive for SGs within these two cell lines are shown below in Figure 4. Over the course of five trials, it was determined that Ars-treated WT cells formed the most SGs on average at 97.98%, with Rsv-treated WT cells forming SGs slightly less often at 89.5%. The untreated and ethanol-treated WT cells formed SGs far less, at an average percent positive of 3.13% and 4.02% respectively. The S51A mutant cells had an average of below 5% positive for all treatment types, which is consistent with the untreated and negative control treatments in the WT cell experiment (Figure 4). There was a significant difference in the average percentage of positive cells between the WT and S51A cells treated with Rsv. While both the untreated and negative control conditions for both cell lines did not contain enough cells producing a positive signal to be considered statistically significant

(below 5%), the positive control (arsenite) and Rsv-treated cells showed great difference between cell types. Starting with the arsenite treated cells, the WT were on average 97.98% positive for SGs, while the S51A cells were only 1.65% positive for SG formation on average between all trials (Figure 4). This significant difference in SG formation is because arsenite SGs are known to be eIF2α-dependent (McEwen et al., 2005). When the ser/ala mutation was made in eIF2α, the protein became unable to phosphorylate, thus causing SG formation to significantly decrease in arsenite treated S51A MEFs (Figure 4).

The S51A Rsv treatment data corresponds with those seen in the S51A arsenite trials. When the S51A cells were acutely exposed to Rsv, the cells produced a 3.56% positive signal between all trials, while the WT cells had an average 89.5% of cells with a positive signal. The average percentage of SG-positive WT cells was slightly decreased when treated with Rsv rather than arsenite (a difference of 8.48%). Overall, the data presented in Figure 4 suggests that Rsv SG formation is eIF2α-dependent in MEFs.

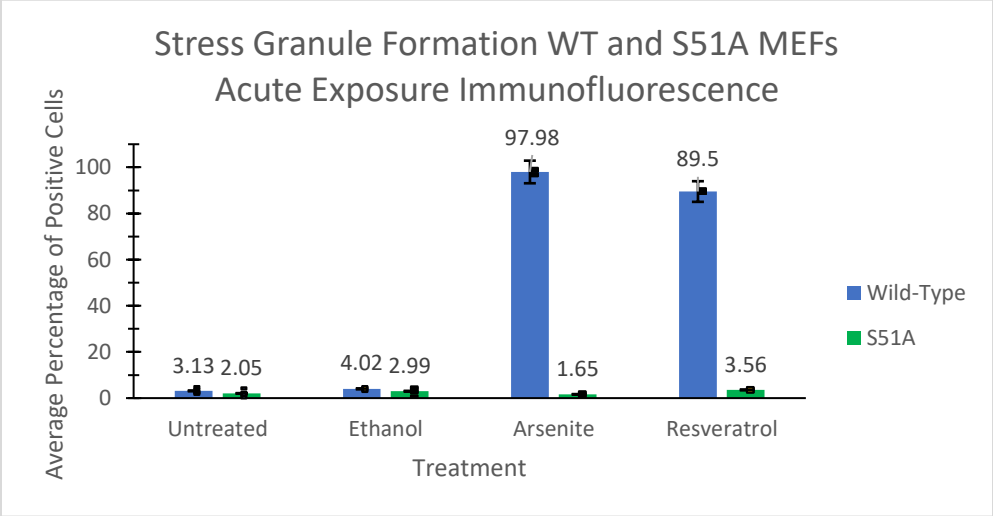

Figure 4. Average percent positive of SG formation in MEF WT and S51A cells. Individual data points indicated by black dots within the bars. The arsenite and Rsv-induced SGs were significantly reduced in S51A MEFs compared to WT cells. Error bars represent standard error of the mean. N=5 for both WT and S51A.

Resveratrol-Induced SGs are Formed Via the eIF2α PERK Kinase

The previous result indicated that Rsv SGs depend on eIF2α phosphorylation to form. In the ISR pathway, only four kinases can lead to the phosphorylation of eIF2α: HRI, PERK, PKR, and GCN2. A previous study hypothesized that PERK kinase is the one that reacts to Rsv exposure to produce SGs in Hap1 cells (Milks et al., 2022). To determine if the same result is

true in adherent MEFs, an acute exposure assay was performed on MEF WT, ΔHRI and ΔPERK cell lines. Figure 5 below displays the results of acute exposure immunoassays on ΔPERK and ΔHRI cells with a new set of WT MEF samples analyzed simultaneously.

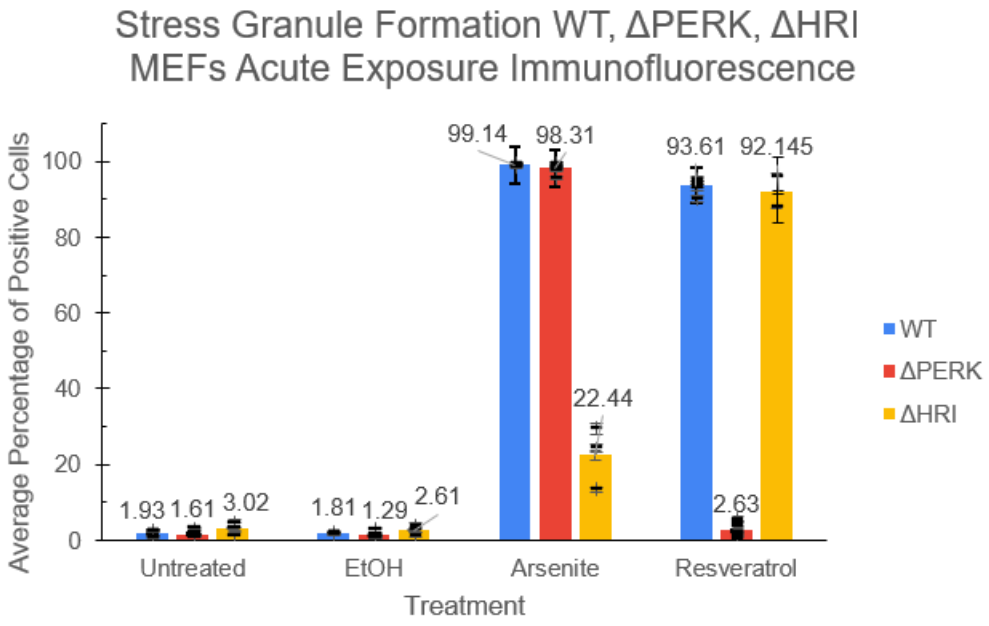

Figure 5. Average percent positive of SG formation in MEF WT, ΔHRI, and ΔPERK cells. Individual data points used to calucalte the displayed averages are indicated by black tick marks. Error bars represent standard error of the mean. WT N=6, ΔPERK N=8, ΔHRI N=3.

According to Figure 5, the untreated and EtOH trials on all three cell types did not produce significant SG formation, with all samples possessing an average percentage of positive cells below 2%. ΔHRI alone showed a reduced percentage of SG formation of 22.44% when exposed to arsenite. The other cell lines had a significantly more positive result, each forming on average more than 90% SGs when treated with arsenite. This supports the prior research that HRI is involved in arsenite SG formation and ISR activation. However the higher-than-usual positive result of arsenite treated ΔHRI cells (22.44%) was unexpected, and could be indicative of compound stresses affecting these cells, or aberrant protein aggregation within these cells.

Of the three cell lines, ΔPERK displayed the least amount of SG formation when exposed to Rsv, possessing an average percent positive of 2.63% between the eight trials analyzed. When the other two tested cell lines, WT and ΔHRI, were treated with Rsv, they formed significantly more SGs. According to Figure 5, the ΔHRI cells were 92.15% positive for SGs over two

replicates, while the WT cells were 93.61% positive for SGs over six replicates. When compared to the ΔPERK results, WT and ΔHRI displayed more than 40 times the amount of SG formation in response to Rsv. These results confirm that Rsv SGs are PERK-dependent in MEFs.

Discussion

The two exposure assays investigated two key questions about the effect of Rsv on cells. Those questions are whether Rsv-induced stress granules form via a dependence on eIF2α phosphorylation, and what ISR kinase does Rsv affect to cause eIF2α phosphorylation. To answer the first question and examine phosphorylation dependence, an eIF2α knockout MEF cell line that replaced amino acid serine51 in the protein with alanine was treated with Rsv and analyzed for SG formation. The resulting cells were compared to Rsv-treated WT cells in order to examine how deactivating eIF2α-mediated translation regulation affected SG formation. It was found that when eIF2α is mutated to prevent phosphorylation, Rsv-induced SG formation decreased significantly along with arsenite-induced SGs, revealing that Rsv SG formation is dependent on eIF2α phosphorylation.

Upon preliminary exposure assay attempts, an interesting phenomenon was observed among the MEF cells treated with Rsv and the negative control EtOH. Prior to treating the cells with 500uM Rsv from a 0.25mM stock (the condition consistent throughout all recorded trials), the WT and S51A cells were treated with 300uM Rsv from a less concentrated 0.10mM stock. This also means that with the 0.10mM stock, 3uL of Rsv and EtOH were added to the corresponding treatment wells instead of the 2uL used with the new stock. When incubating the cells with the larger volume of lower concentration Rsv, both MEF cell types appeared to lose their spindle morphology upon analysis, balling up and lifting from the coverslip. The same phenomenon occurred to the cells treated with 3uL of pure ethanol, the original volume used before reassessment of the treatment concentrations. However, when an Rsv sample was made using less ethanol and applied to the cells at a higher concentration but smaller volume, both cell types did not ball up as they did previously and maintained their spindle-like morphology. This unusual behavior was not observed in the Milks et al. study most likely due to their use of HAP1 suspension cells instead of MEF adherent cells. HAP1 suspension cells are morphologically spherical to begin with, making it more difficult to visualize morphology changes when treated with excess EtOH. This observation suggests that MEF cells have an increased EtOH sensitivity when compared to HAP1 cells that potentially could be due to the adherent nature of MEF cells.

The second exposure assay was performed to investigate if the eIF2α kinase PERK is involved in the Rsv SG formation pathway. This assay utilized two different MEF kinase knockout cell lines, one which removed PERK and the other HRI. The PERK knockout line was

used due to a previous study's experiments suggesting that PERK is far more involved in Rsv SG formation than any of the other three kinases (Milks et al., 2022), while the HRI knockout was used as a control with arsenite since arsenite-induced SGs are proven to use kinase HRI to trigger eIF2α phosphorylation (McEwen et al., 2005). The assay results of both cell lines were compared to WT MEF results to highlight the differences in reaction between the cells. The Rsv acute exposure assay results showed the PERK knockout line to exhibit the smallest percentage of SG formation between the three cell lines tested, possessing an average percent positive of 2.63% between the 8 trials scored. This average percentage is significantly reduced in comparison to the ΔHRI and WT Rsv exposure results, which possessed average percent positives of 92.15% and 93.61%, respectively.

Larger cell death rates were also observed in the Rsv treated ΔPERK cells, the cells shriveling up into spheres and detaching from the coverslip after exposure. This could potentially indicate that the ΔPERK cells could not handle the increased stress due to the lack of SG formation from the loss of the PERK kinase. While we were unable to 100% confirm that Rsv SG formation through eIF2α phosphorylation is solely PERK-dependent, these results did confirm that the PERK kinase plays a significant role in Rsv-induced eIF2α phosphorylation.

The experimental results acquired from this project can contribute to further investigation into Rsv, PERK, and their relationship with eIF2α in mammalian cells. Future continuations of this study could involve performing western blot assays of the two exposure experiments. This was an experiment performed by Milks et al. in their research on Rsv-induced SG formation in HAP1 cells, where they found their kinase knockout acute exposure assay and the Western Blot of those cells produced conflicting evidence on the involvement of PERK. Performing a western blot on the cells from this study would confirm if PERK is solely involved in Rsv induced eIF2α activation.

Another next step from this study could involve further research into the conflict between these results collected and those shown in Amen et al., 2021, which suggested that Rsv does not induce phosphorylation of eIF2α as much as arsenite does. Their results suggest that Rsv SGs potentially could be formed through an auxiliary pathway that is faster than the arsenite SG pathway, which is in direct conflict with the exposure assay results from both this and the Milks et al. projects. Future experiments to better understand how Rsv induces stress granules could include an acute exposure assay on a mutated cell line with both the eIF2α S51A inactivation

mutation and the removal of the PERK kinase. By blocking both the potential phosphorylating kinase and the phosphorylation site in the protein there would be absolutely no phosphorylation of eIF2α, so if no SGs it would confirm PERK's involvement in the activation pathway.

While great care was taken to avoid errors, there were a few encountered throughout the research process. One source of error was due to the fragility of the cells once thawed from their cryotubes. Upon thawing the ΔHRI and S51A cells, there was very little to no cell growth and proliferation. The cells were extremely fragile and difficult to keep healthy and uncontaminated. The ΔHRI cells in particular had cell walls that were easier to break than any other cell line used, and at one point the cell line had to be completely revived from a single surviving cell. It was not uncommon for the ΔHRI cells to die during the treatment and staining process, causing a decrease in the replicate samples recorded for the ΔHRI trials. Another potential error source came from the method used to score cells. Only a selection of cells from each sample could be analyzed using the fluorescence microscope. It would be impossible to accurately count and sort every cell in a sample into a positive or negative result. By scoring a sample of cells from each slide there was the potential that the frames analyzed were not wholly representative of all cells on the slide.

References

Amen, T., Guihur, A., Zelent, C., Ursache, R., Wilting, J., & Kaganovich, D. (2021). Resveratrol and related stilbene-derivatives induce Stress Granules with distinct clearance kinetics. *Molecular Biology of the Cell*, mbc.E21-02-0066. https://doi.org/10.1091/mbc.E21-02-0066

Anderson, P., & Kedersha, N. (2009). Stress granules. *Current Biology*, *19*(10), R397–R398. https://doi.org/10.1016/j.cub.2009.03.013

Bansal, M., Singh, N., Pal, S., Dev, I., & Ansari, K. M. (2018). Chapter three—Chemopreventive role of dietary phytochemicals in colorectal cancer. In J. C. Fishbein & J. M. Heilman (Eds.), *Advances in Molecular Toxicology* (Vol. 12, pp. 69–121). Elsevier. https://doi.org/10.1016/B978-0-444-64199-1.00004-X

Beigl, T. B., Kjosås, I., Seljeseth, E., Glomnes, N., & Aksnes, H. (2020). Efficient and crucial quality control of HAP1 cell ploidy status. *Biology Open*, *9*(11), bio057174. https://doi.org/10.1242/bio.057174

Campos-Melo, D., Hawley, Z. C. E., Droppelmann, C. A., & Strong, M. J. (2021). The integral role of rna in stress granule formation and function. *Frontiers in Cell and Developmental Biology*, *9*, 621779. https://doi.org/10.3389/fcell.2021.621779

Darini, C., Ghaddar, N., Chabot, C. *et al.* An integrated stress response via PKR suppresses HER2+ cancers and improves trastuzumab therapy. *Nat Commun* 10, 2139 (2019). https://doi.org/10.1038/s41467-019-10138-8

Frémont, L. (2000). Biological effects of resveratrol. *Life Sciences*, *66*(8), 663-673. https://doi.org/10.1016/S0024-3205(99)00410-5

Fulda, S., Gorman, A. M., Hori, O., & Samali, A. (2010). Cellular stress responses: cell survival and cell death. *International Journal of Cell Biology*, *2010*, 214074. https://doi.org/10.1155/2010/214074

Han, A.-P. (2001). Heme-regulated eIF2α kinase (HRI) is required for translational regulation and survival of erythroid precursors in iron deficiency. *The EMBO Journal*, *20*(23), 6909–6918. https://doi.org/10.1093/emboj/20.23.6909

Harding, H. P., Zhang, Y., Bertolotti, A., Zeng, H., & Ron, D. (2000). *Perk* is essential for translational regulation and cell survival during the unfolded protein response. *Molecular Cell*, *5*(5), 897–904. https://doi.org/10.1016/S1097-2765(00)80330-5

Kedersha, N., Panas, M.D., Achorn, C.A., Lyons, S., Tisdale, S., Hickman, T., Thomas, M., Lieberman, J., McInerney, G.M., Ivanov, P. and Anderson, P. (2016). G3BP–Caprin1–USP10 complexes mediate stress granule condensation and associate with 40S subunits. *Journal of Cell Biology*, 212(7). https://doi.org/10.1083/jcb.201508028

Koromilas, A. E. (2019). M(en)TORship lessons on life and death by the integrated stress response. *Biochemica et Biophysica Acta (BBA) – General Subjects*, *1863*(3), 644-649. https://doi.org/10.1016/j.bbagen.2018.12.009

Langcake, P., & Pryce, R. J. (1976). The production of resveratrol by Vitis vinifera and other members of the Vitaceae as a response to infection or injury. *Physiological Plant Pathology*, *9*(1), 77–86. https://doi.org/10.1016/0048-4059(76)90077-1

Matsuki, H., Takahashi, M., Higuchi, M., Makokha, G. N., Oie, M., & Fujii, M. (2013). Both G3BP1 and G3BP2 contribute to stress granule formation. *Genes to Cells*, *18*(2), 135-146. https://doi.org/10.1111/gtc.12023

McEwen, E., Kedersha, N., Song, B., Scheuner, D., Gilks, N., Han, A., Chen, J.-J., Anderson, P., & Kaufman, R. J. (2005). Heme-regulated inhibitor kinase-mediated phosphorylation of eukaryotic translation initiation factor 2 inhibits translation, induces stress granule formation, and mediates survival upon arsenite exposure. *Journal of Biological Chemistry*, *280*(17), 16925–16933. https://doi.org/10.1074/jbc.M412882200

Milks, J., Kola, M., Staples, M., & Wall, A. (2022). PERK up! Resveratrol-Induced Stress Granules Involve PERK Pathway Activation. Major Qualifying Project. Worcester Polytechnic Institute, Worcester, MA. Available from: https://digital.wpi.edu/concern/student_works/z316q4953?locale=en

Piotrowska, H., Kucinska, M., & Murias, M. (2012). Biological activity of piceatannol: Leaving the shadow of resveratrol. *Mutation Research/Reviews in Mutation Research*, *750*(1), 60–82. https://doi.org/10.1016/j.mrrev.2011.11.001

Pizarro, J. G., Verdaguer, E., Ancrenaz, V. et al. (2011). Resveratrol inhibits proliferation and promotes apoptosis of neuroblastoma cells: role of Sirtuin 1. *Neurochem Res* 36, 187-194 (2011). https://doi.org/10.1007/s11064-010-0296-y

Scheuner, D., Song, B., McEwen, E., Liu, C., Laybutt, R., Gillespie, P., Saunders, T., Bonner-Weir, S., & Kaufman, R. J. (2001). Translational control is required for the unfolded protein response and in vivo glucose homeostasis. *Molecular Cell*, *7*(6), 1165–1176. https://doi.org/10.1016/S1097-2765(01)00265-9

Tourrière, H., K. Chebli, L. Zekri, B. Courselaud, J.M. Blanchard, E. Bertrand, and J. Tazi. (2003). The RasGAP-associated endoribonuclease G3BP assembles stress granules. *J. Cell Biol*. 160:823–831. https://doi.org/10.1083/jcb.200212128

Takashina, M., Inoue, S., Tomihara, K., Tomita, K., Hattori, K., Zhao, Q. ... Hattori, Y. (2017). Different effect of resveratrol to induction of apoptosis depending on the type of human cancer cells. *International Journal of Oncology*, 50, 787-797. https://doi.org/10.3892/ijo.2017.3859

Villa-Cuestra, E., Boylan, J. M., Tatar, M., & Gruppuso, P. A. (2011). Resveratrol inhibits protein translation in hepatic cells. *PLOS ONE, 6*(12), e29513. https://doi.org/10.1371/journal.pone.0029513

Appendix A: S51A and WT MEF Acute Exposure Assay Raw Data

Trial 1:

Condition	Yes	No	Total	% Positive
WT untreated	7	270	277	2.53%
WT EtOH	9	278	287	3.14%
WT Arsenite	283	10	293	96.59%
WT Resveratrol	324	35	359	90.25%
S51A untreated	1	305	306	0.33%
S51A EtOH	2	280	282	0.71%
S51A Arsenite	2	321	323	0.62%
S51A Resveratrol	9	284	293	3.07%

Trial 2:

Condition	Yes	No	Total	% Positive
WT untreated	21	420	441	4.76%
WT EtOH	17	362	379	4.49%
WT Arsenite	302	4	306	98.69%
WT Resveratrol	346	43	389	88.95%
S51A untreated	16	364	380	4.21%
S51A EtOH	17	357	374	4.55%
S51A Arsenite	8	345	353	2.27%
S51A Resveratrol	16	406	422	3.79%

Trial 3:

Condition	Yes	No	Total	% Positive
WT untreated	19	497	516	3.68%
WT EtOH	15	354	369	4.07%
WT Arsenite	359	5	364	98.63%
WT Resveratrol	401	43	444	90.32%
S51A untreated	5	326	331	1.51%
S51A EtOH	11	365	376	2.93%
S51A Arsenite	8	336	344	2.33%
S51A Resveratrol	19	482	501	3.79%

Trial 4:

Condition	Yes	No	Total	% Positive
WT untreated	13	458	471	2.76%
WT EtOH	16	435	451	3.55%
WT Arsenite	425	14	439	96.81%
WT Resveratrol	519	64	583	89.02%
S51A untreated	13	532	545	2.39%
S51A EtOH	15	344	359	4.18%
S51A Arsenite	5	292	297	1.68%
S51A Resveratrol	19	428	447	4.25%

Trial 5:

Condition	Yes	No	Total	% Positive
WT untreated	7	357	364	1.92%
WT EtOH	17	332	349	4.87%
WT Arsenite	359	3	362	99.17%
WT Resveratrol	375	46	421	89.07%
S51A untreated	6	323	329	1.82%
S51A EtOH	10	374	384	2.60%
S51A Arsenite	5	362	367	1.36%
S51A Resveratrol	11	370	381	2.89%

WT Averages				
% + of...	**WT Untreated**	**WT Ethanol**	**WT Arsenite**	**WT Resveratrol**
Trial1	2.53	3.14	96.59	90.25
Trial2	4.76	4.49	98.69	88.95
Trial3	3.68	4.07	98.63	90.32
Trial4	2.76	3.55	96.81	89.02
Trial5	1.92	4.87	99.17	89.07
Average	3.13	4.02	97.98	89.5
St. Dev.	1.109098733	0.696620413	1.187821535	0.698262128

S51A Averages				
% + of...	**S51A Untreated**	**S51A Ethanol**	**S51A Arsenite**	**S51A Resveratrol**
Trial1	0.33	0.71	0.62	3.07
Trial2	4.21	4.55	2.27	3.79
Trial3	1.51	2.93	2.33	3.79
Trial4	2.39	4.18	1.68	4.25
Trial5	1.82	2.60	1.36	2.89
Average	2.05	2.99	1.65	3.56
St. Dev.	1.42162583	1.51688167	0.70581159	0.563666568

Appendix B: ΔHRI, ΔPERK, and WT MEF Acute Assay Raw Data

WT Trials				
Sample	**Yes**	**No**	**Total**	**% Positive**
220726 untreated	3	429	432	0.69
220726 EtOH	6	378	384	1.56
220726 Ars	452	2	454	99.56
220726 Rsv	318	35	353	90.08
220729 untreated	11	467	478	2.30
220729 EtOH	8	417	425	1.88
220729 Ars	404	3	407	99.26
220729 Rsv	374	20	394	94.92
220803 untreated	10	416	426	2.35
220803 EtOH	8	370	378	2.12
220803 Ars	329	4	333	98.80
220803 Rsv	385	25	410	93.90
220805 untreated	3	315	318	0.94
220805 EtOH	6	379	385	1.56
220805 Ars	355	5	360	98.61
220805 Rsv	395	19	414	95.41
220810A untreated	11	405	416	2.64
220810B untreated	9	332	341	2.64
220810A EtOH	6	313	319	1.88
220810B EtOH	7	372	379	1.85
220810A Ars	364	3	367	99.18
220810B Ars	338	2	340	99.41
220810A Rsv	387	28	415	93.25
220810B Rsv	429	27	456	94.08

PERK trials

Sample	Yes	No	Total	% Positive
220726 untreated	3	317	320	0.94
220726 EtOH	2	276	278	0.72
220726 Ars	319	15	334	95.51
220726 Rsv	2	409	411	0.49
220802A untreated	5	349	354	1.41
220802A EtOH	6	368	374	1.60
220802A Ars	387	3	390	99.23
220802A Rsv	8	396	404	1.98
220802B untreated	6	398	404	1.49
220802B EtOH	3	402	405	0.74
220802B Ars	337	6	343	98.25
220802B Rsv	11	508	519	2.12
220803 untreated	13	393	406	3.20
220803 EtOH	11	349	360	3.06
220803 Ars	381	8	389	97.94
220803 Rsv	14	300	314	4.46
220805A untreated	4	330	334	1.20
220805A EtOH	3	358	361	0.83
220805A Ars	373	2	375	99.47
220805A Rsv	14	350	364	3.85
220805B untreated	4	323	327	1.22
220805B EtOH	4	337	341	1.17
220805B Ars	400	6	406	98.52
220805B Rsv	20	344	364	5.49
220810A untreated	5	376	381	1.31
220810B untreated	7	326	333	2.10
220810A EtOH	4	379	383	1.04
220810B EtOH	4	349	353	1.13
220810A Ars	489	3	492	99.39
220810B Ars	380	7	387	98.19

HRI Trials

Sample	Yes	No	Total	% Positive
220729 untreated	15	318	333	4.50
220729 EtOH	13	337	350	3.71
220729 Ars	119	284	403	29.53
220729 Rsv	360	14	374	96.26
220909 untreated	4	360	364	1.10
220909 EtOH	10	344	354	2.82
220909 Ars	111	345	456	24.34
220909 Rsv	331	45	376	88.03
220726 untreated	10	280	290	3.45
220726 EtOH	4	304	308	1.30
220726 Ars	46	296	342	13.45

WT Averages				
% + of…	**WT untreated**	**WT EtOH**	**WT Ars**	**WT Rsv**
Sample 1	0.69	1.56	99.56	90.08
Sample 2	2.3	1.88	99.26	94.92
Sample 3	2.35	2.12	98.8	93.9
Sample 4	0.94	1.56	98.61	95.41
Sample 5	2.64	1.88	99.18	93.25
Sample 6	2.64	1.85	99.41	94.08
Average	1.926666667	1.808333333	99.1366667	93.60666667
St. Dev.	0.876257192	0.215630857	0.36379481	1.889525514
PERK Averages				
% + of…	**ΔPERK untreated**	**ΔPERK EtOH**	**ΔPERK Ars**	**ΔPERK Rsv**
Trial 1	0.94	0.72	95.51	0.46
Trial 2	1.41	1.6	99.23	1.98
Trial 3	1.49	0.74	98.25	2.12
Trial 4	3.2	3.06	97.94	4.46
Trial 5	1.2	0.83	99.47	3.85
Trial 6	1.22	1.17	98.52	5.49
Trial 7	1.31	1.04	99.39	1.45
Trial 8	2.1	1.13	98.19	1.24
Average	1.60875	1.28625	98.3125	2.63125
St. Dev.	0.725227797	0.771861155	1.27600661	1.762015384

HRI Trials				
% + of…	**ΔHRI untreated**	**ΔHRI EtOH**	**ΔHRI Ars**	**ΔHRI Rsv**
Sample 1	4.5	3.71	29.53	96.26
Sample 2	1.1	2.82	24.34	88.03
Sample 3	3.45	1.3	13.45	
Average	3.016666667	2.61	22.44	92.145
St. Dev.	1.740928871	1.218646791	8.206649743	5.819488809